

Supplementary Information: Drought sensitivity is not a species trait: Tropical tree drought sensitivity is jointly shaped by drought characteristics, species adaptations, and individual microenvironments

Contents

Study site	2
Climate data and correlations	3
Data cleaning additional methods	5
Growth timeseries and anomalies	6
Drought year growth of species and individuals	8
Variables and their distributions	11
Raw sensitivity and residuals with predictors	12
Conditional dependencies	17
Alternate models using Topographic Position Index	21
Alternate model using species random effect only on intercept	23
Alternate models as causal inquiries following backdoor criteria	24
References	24
Authors	
Krishna Anujan ^{1,2*} ORCiD: 0000-0003-3604-5895	
Sean McMahon ^{2,3} ORCiD: 0000-0001-8302-6908	
Sarayudh Bunyavejchewin ⁴ ORCiD: 0000-0002-1976-5041	
Stuart J. Davies ³ ORCiD: 0000-0002-8596-7522	
Helene C. Muller-Landau ³ ORCiD : 0000-0002-3526-9021	
Nantachai Pongpattananurak ⁵ ORCiD: 0000-0001-8687-6182	
Kristina Anderson-Teixeira ^{1,3} ORCiD: 0000-0001-8461-9713	

Study site



Figure S1: Representative photographs of the 50-ha long-term monitoring site in Huai Kha Khaeng Thailand, with dendrometer banded trees. Photo credits: left image: Sarayudh Bunyavejchewin, right image: Krishna Anujan

Climate data and correlations

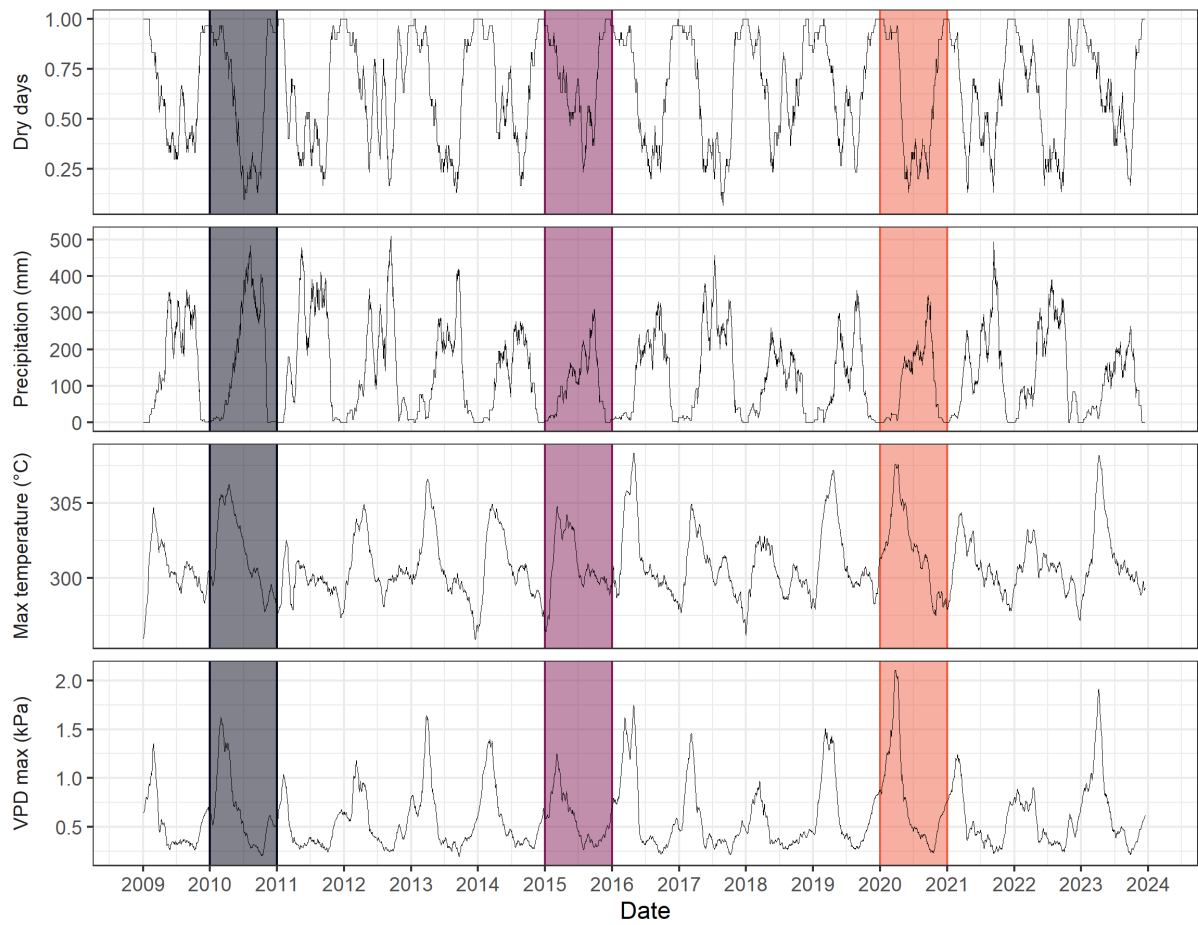


Figure S2: Raw climate data timeseries from 2009 to 2023 from ERA5Land and CHIRPS. Measurements represent daily rolling means over a 30-day time window for precipitation, max temperature and VPD and rolling sum for number of dry days. The shaded areas indicate the three drought years analysed - 2010, 2015 and 2020. Dry-season in the region is typically from November to April.

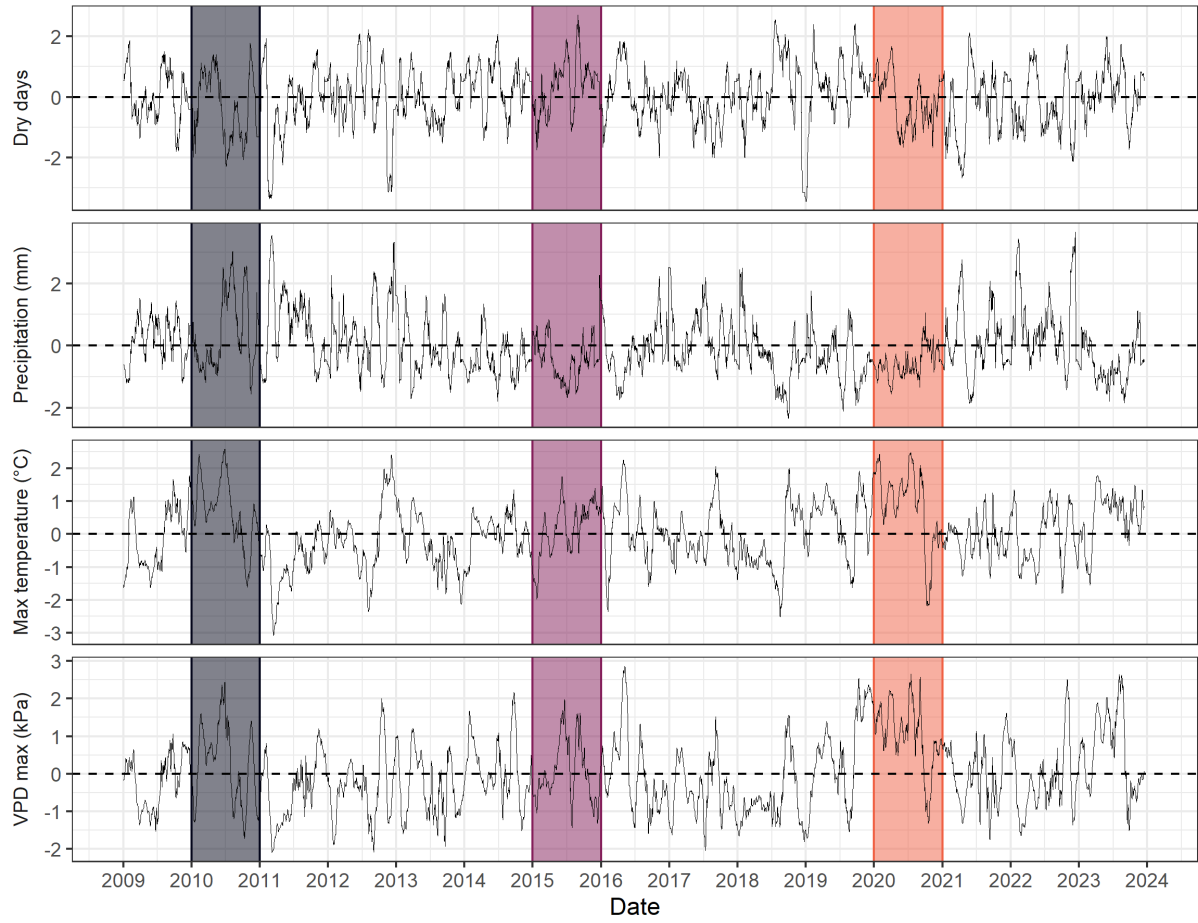


Figure S3: Climate anomalies for all variables from 2009 to 2020. Values represent number of standard deviations from the long-term mean for daily rolling mean values. The shaded areas indicate the three drought years analysed - 2010, 2015 and 2020. Dry-season in the region is typically from November to April.

Data cleaning additional methods

For raw measurements of dendrometer band window size, we conducted QAQC steps as follows: 1. Removed potentially misidentified individuals. We removed individuals with conflicting metadata on tag or location across censuses. We did not remove individuals with conflicting species identification because these are often updated during the ForestGEO censuses. Therefore, we used the latest version of species identification for each tag shared by the PIs of the HKK plot. 2. Removed potential misidentified bands. Each new dendroband installed on a tree is numbered sequentially starting from 1. We removed any measurements made on bands old bands after a new band series had begun. 3. Removing measurements that appeared likely to be data entry errors. We identified misplaced decimals by checking if the ratio between adjacent window size measurements were closer to 1 or 10 or 100. We removed measurements that had ratios closer to 10 or 100 than 1, assuming that these were likely misplaced decimals.

After calculating DBH from window size measurements and calculating annualised growth increments, we conducted further QAQC on these increments to create the final dataset: 1. We excluded large measurement outliers, defined as > 3 standard deviations from the mean increment across all observations. 2. We excluded trees with negative increments or increments close to zero over the whole timeseries of observations. These low growing trees may be indicative of stress or mortality, and likely to bias analysis of interannual growth variation. 3. We used concurrent tape measurements on dendrobanded trees to flag likely errors. We calculated annualised increments from annual tape measurements made on each dendrobanded tree at each census, using similar methods as described for dendrometer bands. For each tree and year, we calculated the degree of deviation of these measurements from each other as the Euclidean distance from the 1:1 line. We found that 90% of the increments were within 5 mm of deviation, which we retained as a high confidence dataset. We excluded the remaining 10% from the analysis, although we were unable to ascertain whether the discrepancy was because of errors in tape or dendroband measurements.

Growth timeseries and anomalies

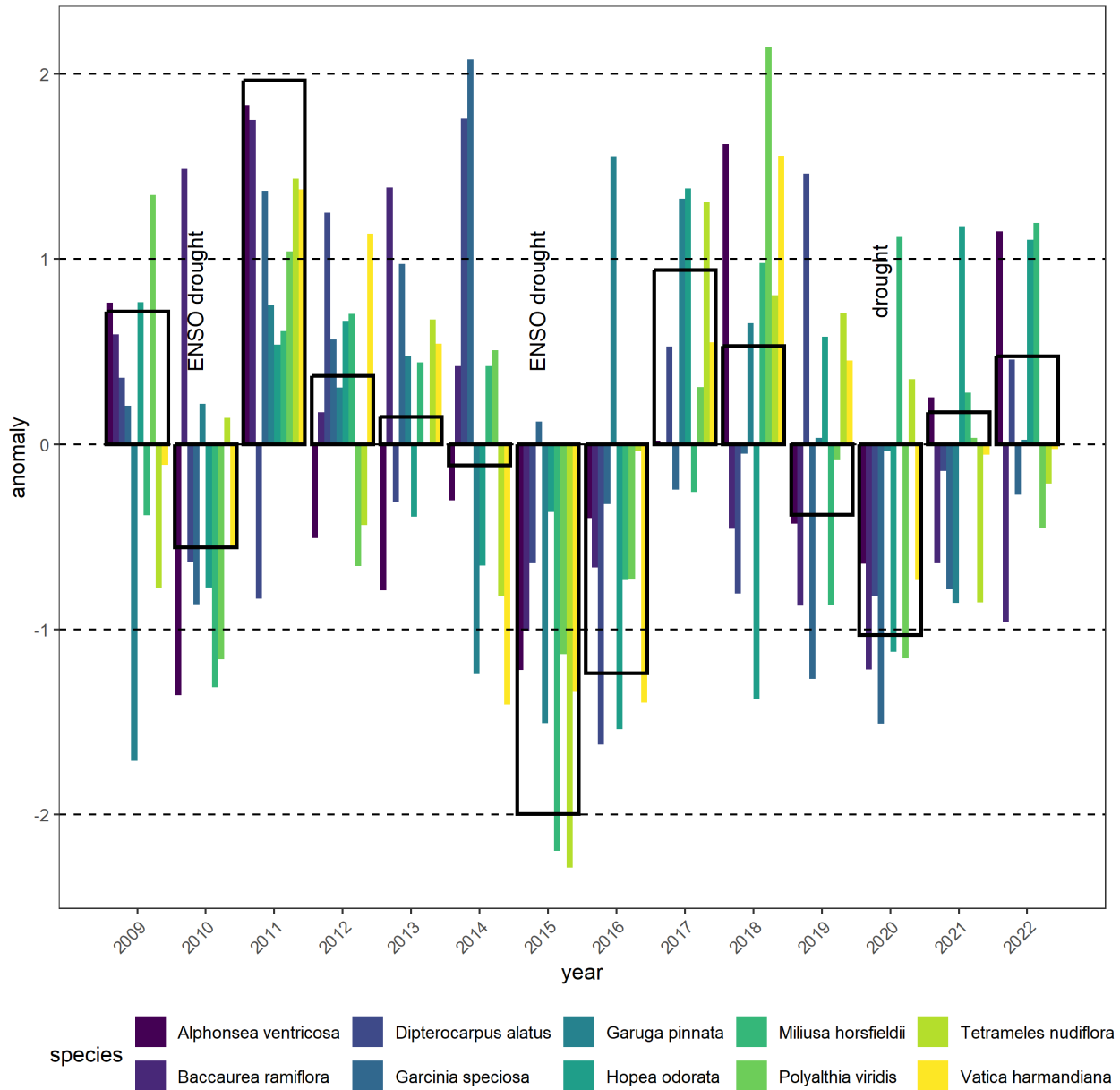


Figure S4: Growth anomalies across the timeseries. Growth anomalies for each year calculated as the number of standard deviations in growth each year from mean growth across all years and summarised for plot and species.

Drought year growth of species and individuals

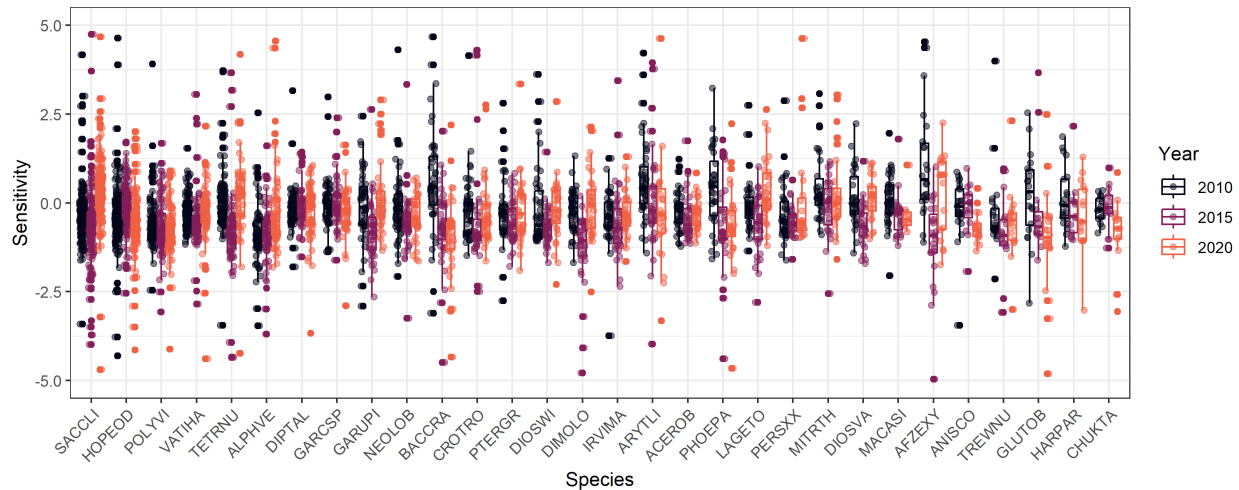


Figure S5: Species sensitivities in drought years 2010, 2015 and 2020. Boxplots represent 25th, 50th (median) and 75th percentile of sensitivity for each species in each year and whiskers represent 95% CIs. All individual sensitivities represented by jittered points.

Table S1: Species characteristics and their median sensitivities for the three drought years. Species characteristics reported include accepted scientific names of species analysed, their ForestGEO codes, deciduousness values (amount of leaf loss at maximum) and IUCN status as accessed in September 2025. For each species, median growth sensitivity +/- standard deviation is reported across the individuals analysed in 2010, 2015, and 2020 - the three drought years considered. IUCN category codes - “EN” = Endangered, “VU” = Vulnerable, “LC” = Least Concern, “DD” = Data Deficient. Empty columns indicate species which were not part of the IUCN assessment.

Species code	Species name	IUCN		2010	2015	2020
		deciduousness	status			
ACEROB	Acer oblongum	1.780	LC	-0.2 +/- 0.56	-0.61 +/- 0.65	-0.31 +/- 0.46
AFZEXY	Afzelia xylocarpa	3.780	EN	0.65 +/- 1.55	-0.92 +/- 1.26	0.77 +/- 1.81
ALPHVE	Alphonsea ventricosa	NA	DD	-0.94 +/- 0.89	-0.85 +/- 1.01	-0.51 +/- 1.21
ANISCO	Anisoptera costata	1.220	EN	-0.1 +/- 0.88	0 +/- 0.69	-0.76 +/- 0.45
ARYTLI	Arytera littoralis	0.220	LC	0.43 +/- 1.13	-0.21 +/- 1.45	-0.37 +/- 1.73
BACCRA	Baccaurea ramiflora	0.250	LC	0.43 +/- 1.37	-0.7 +/- 1.05	-0.72 +/- 1.16
CHUKTA	Chukrasia tabularis	1.890	LC	-0.2 +/- 0.36	-0.13 +/- 0.65	-0.73 +/- 1.03
CROTRO	Croton roxburghii	0.486	LC	-0.2 +/- 0.91	-0.92 +/- 1.36	-0.49 +/- 0.93
DIMOLO	Dimocarpus longan	0.290	DD	-0.14 +/- 0.61	-1.06 +/- 1.05	-0.06 +/- 0.95
DIOSVA	Diospyros variegata	0.160		-0.03 +/- 0.82	-0.67 +/- 0.63	0.18 +/- 0.61

Species code	Species name	IUCN		2010	2015	2020
		deciduousness	status			
DIOSWI	Diospyros winitii	1.570		-0.63 +/- 1.14	-0.73 +/- 0.52	-0.21 +/- 0.89
DIPTAL	Dipterocarpus alatus	1.350	VU	-0.2 +/- 0.58	-0.16 +/- 0.66	-0.1 +/- 0.82
GARCSP	Garcinia speciosa	0.340		-0.08 +/- 0.7	-0.16 +/- 0.75	-0.22 +/- 0.71
GARUPI	Garuga pinnata	3.970	LC	-0.13 +/- 1.02	-0.83 +/- 0.88	-0.07 +/- 1.29
GLUTOB	Gluta obovata	0.380		0.32 +/- 1.24	-0.78 +/- 1.97	-0.98 +/- 1.53
HARPAR	Harpullia arborea	0.660	LC	-0.08 +/- 0.86	-0.38 +/- 0.84	-0.53 +/- 1.04
HOPEOD	Hopea odorata	0.720	VU	-0.46 +/- 0.8	-0.08 +/- 0.65	-0.58 +/- 0.84
IRVIMA	Irvingia malayana	0.510	LC	-0.39 +/- 0.79	-0.72 +/- 1.05	-0.39 +/- 0.61
LAGETO	Lagerstroemia tomentosa	3.650		-0.17 +/- 0.75	-0.56 +/- 0.82	0.1 +/- 1.31
MACASI	Macaranga siamensis	NA	LC	0.08 +/- 0.69	-0.28 +/- 0.58	-0.48 +/- 0.56
MITRTH	Mitraphora thorelii	0.480	LC	0.16 +/- 0.97	0.02 +/- 0.81	-0.02 +/- 1.13
NEOLOB	Neolitsea obtusifolia	0.210		-0.2 +/- 0.97	-0.57 +/- 0.9	-0.44 +/- 0.62
PERSXX	Persea sp.	0.080		-0.54 +/- 0.81	-0.57 +/- 0.46	-0.56 +/- 1.83
PHOEPA	Phoebe paniculata	0.240	LC	0.45 +/- 1.12	-0.83 +/- 1.27	-0.75 +/- 1.14
POLYVI	Polyalthia viridis	1.620		-0.76 +/- 0.74	-0.76 +/- 0.77	-0.81 +/- 0.71
PTERGR	Pterospermum grandiflorum	3.880	LC	-0.29 +/- 1	-0.64 +/- 0.61	-0.31 +/- 0.93
SACCLI	Miliusa horsfieldii	3.385	LC	-0.39 +/- 0.79	-0.54 +/- 0.99	0.35 +/- 1.19
TETRNU	Tetrameles nudiflora	4.000	LC	-0.14 +/- 0.85	-0.9 +/- 1.24	0.22 +/- 1.1
TREWNU	Trewia nudiflora	3.600	LC	-0.68 +/- 1.17	-0.92 +/- 1.18	-0.49 +/- 1.03
VATIHA	Vatica harmandiana	0.492	DD	-0.22 +/- 0.52	-0.56 +/- 0.85	-0.22 +/- 0.84

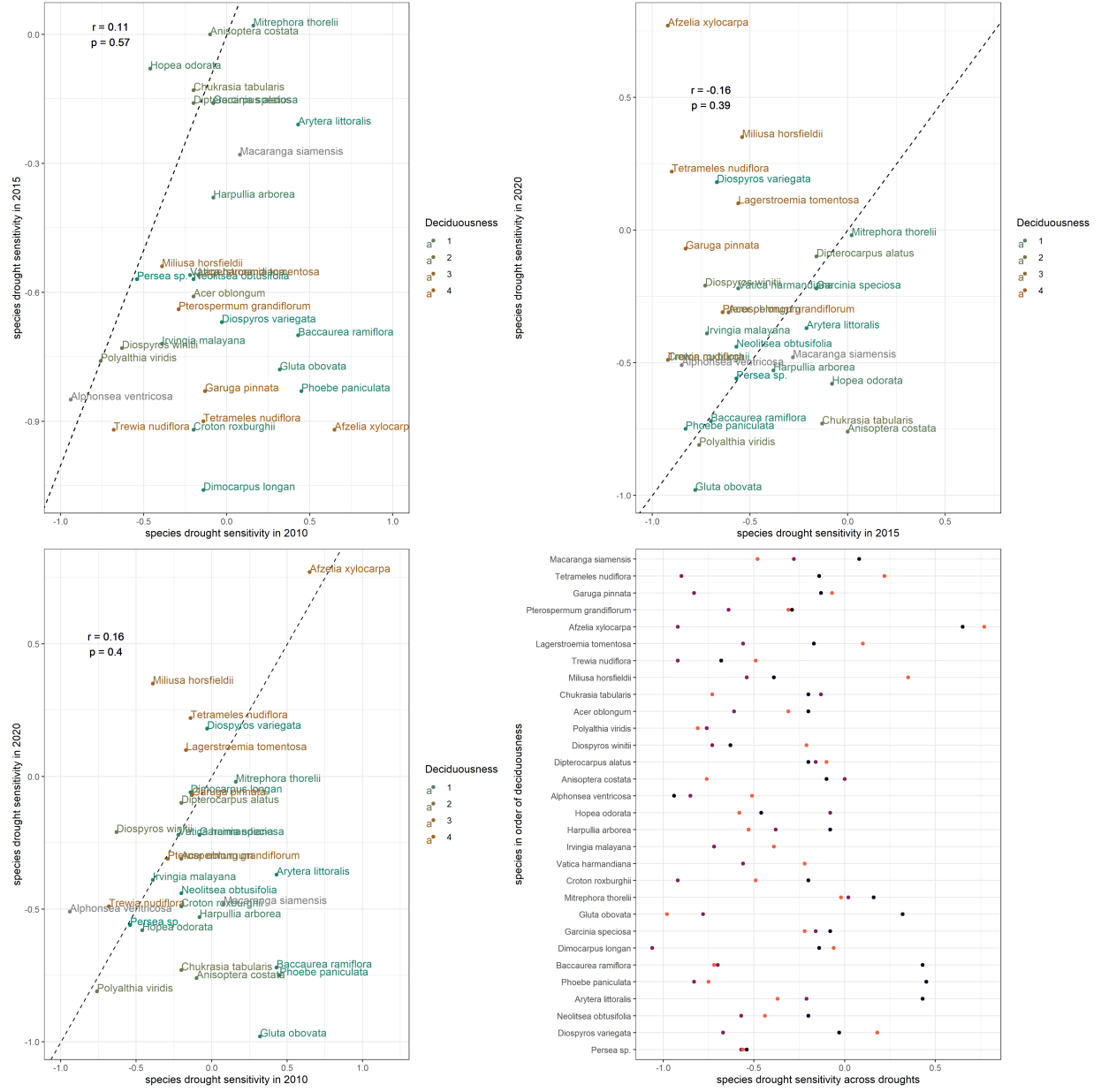


Figure S6: Correlations of species sensitivities across the two years. The top-left panel shows correlation of species median sensitivities and Pearson's correlation coefficient in the 2010 and 2015, top right shows 2010 and 2020, and bottom left shows 2015 and 2020. Colour gradient represents deciduousness scale and dotted line is the 1:1 line. The bottom right panel shows how species drought sensitivities varies among the three years; the color scheme for droughts matches that in main text figure 1.

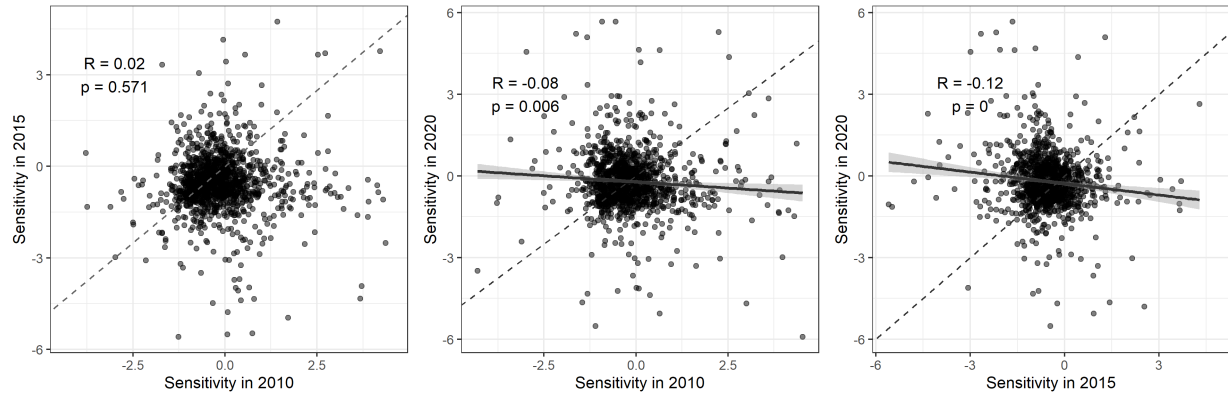


Figure S7: Correlation of individual sensitivities across the two years along with Pearson's correlation coefficient and the 1:1 line.

Variables and their distributions

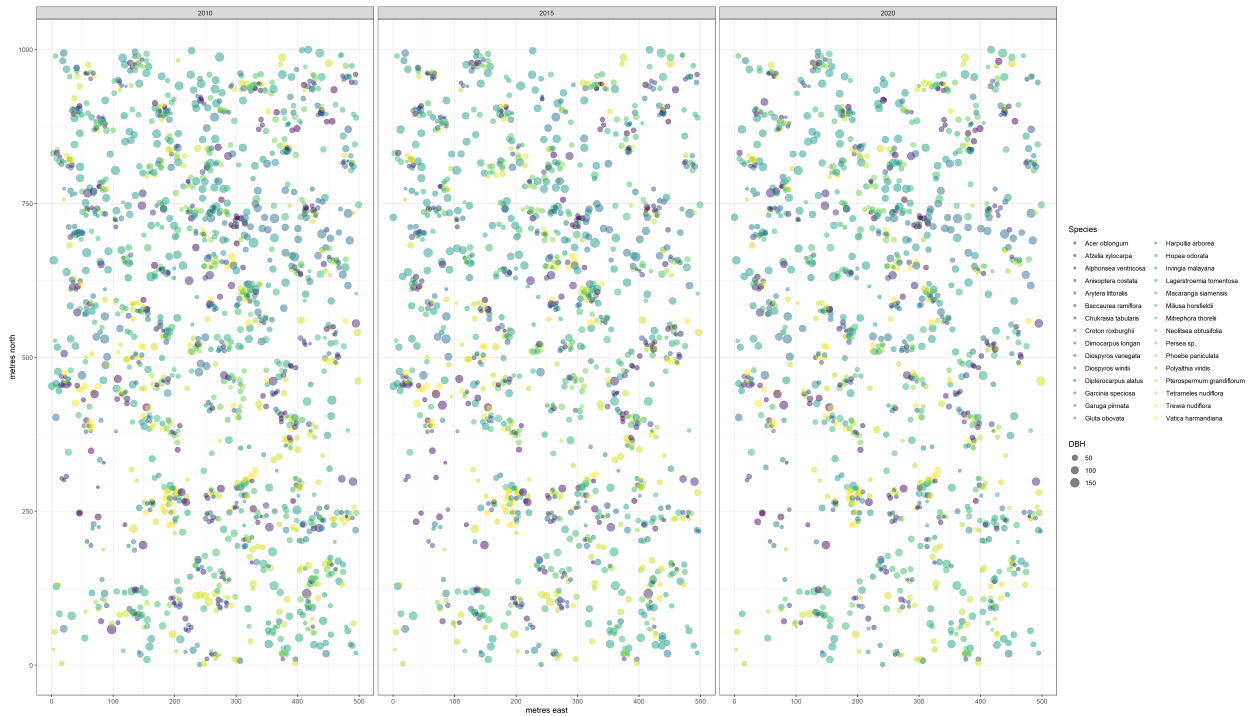


Figure S8: Map of trees with dendrobands in HKK, included in analyses in the 2010, 2015 and 2020 datasets

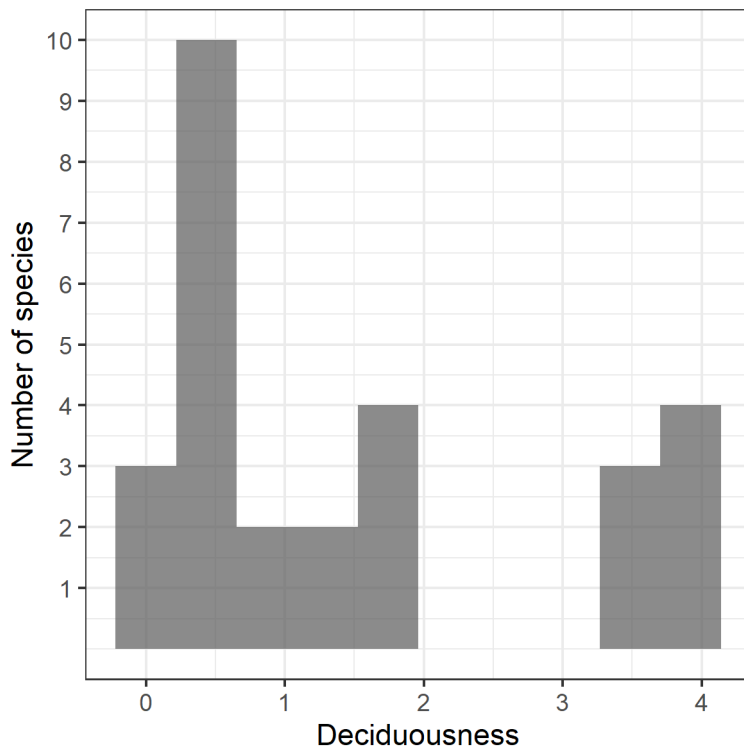


Figure S9: Distribution of deciduousness values among the 30 species analysed

Raw sensitivity and residuals with predictors

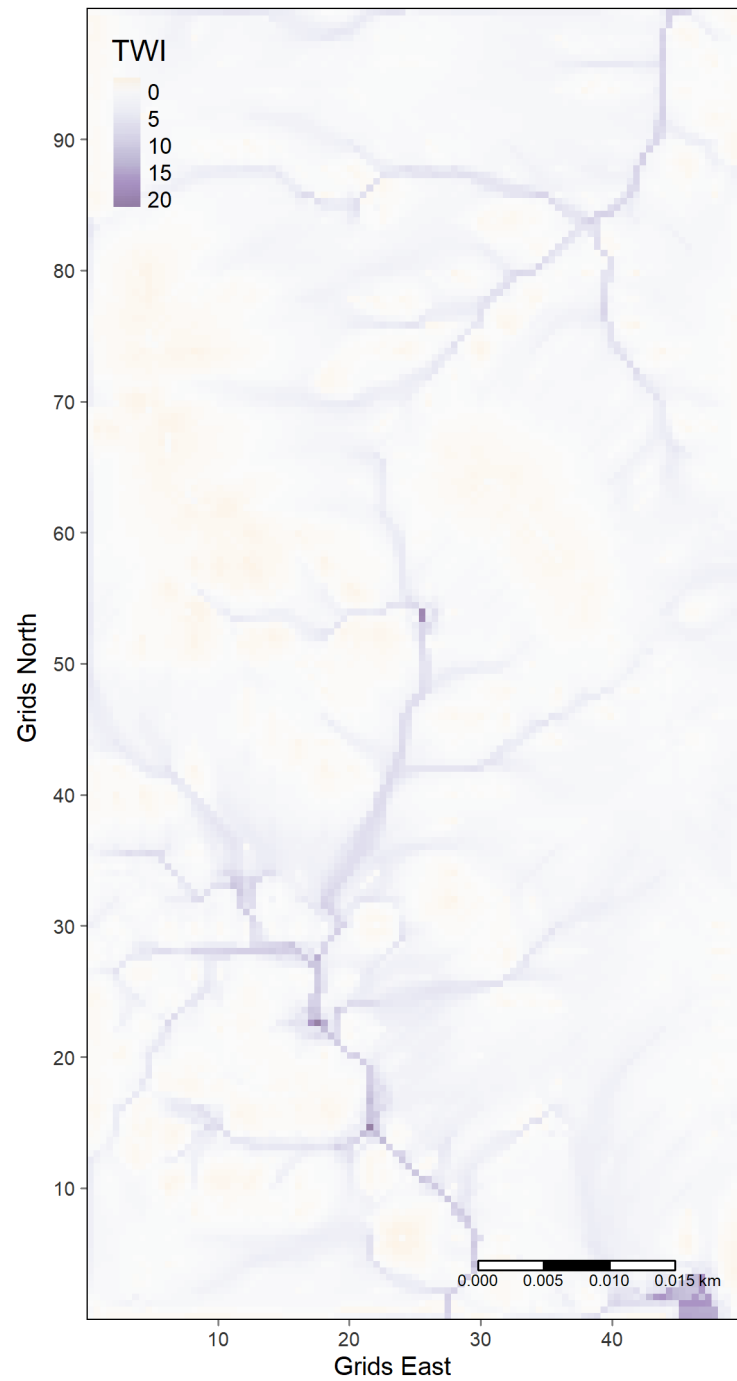


Figure S10: Calculated Topographic Wetness Index (TWI) values for the HKK plot

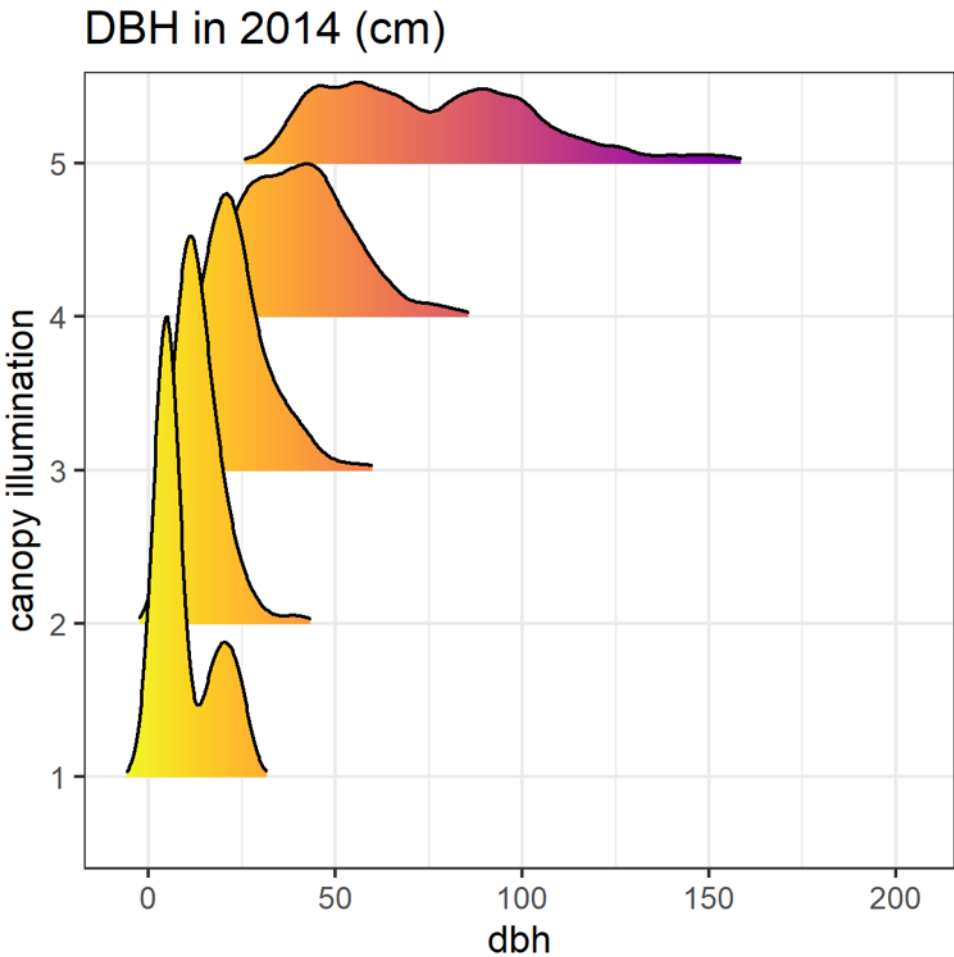


Figure S11: Distribution of DBH with Crown Illumination Index (CII) in 2014.

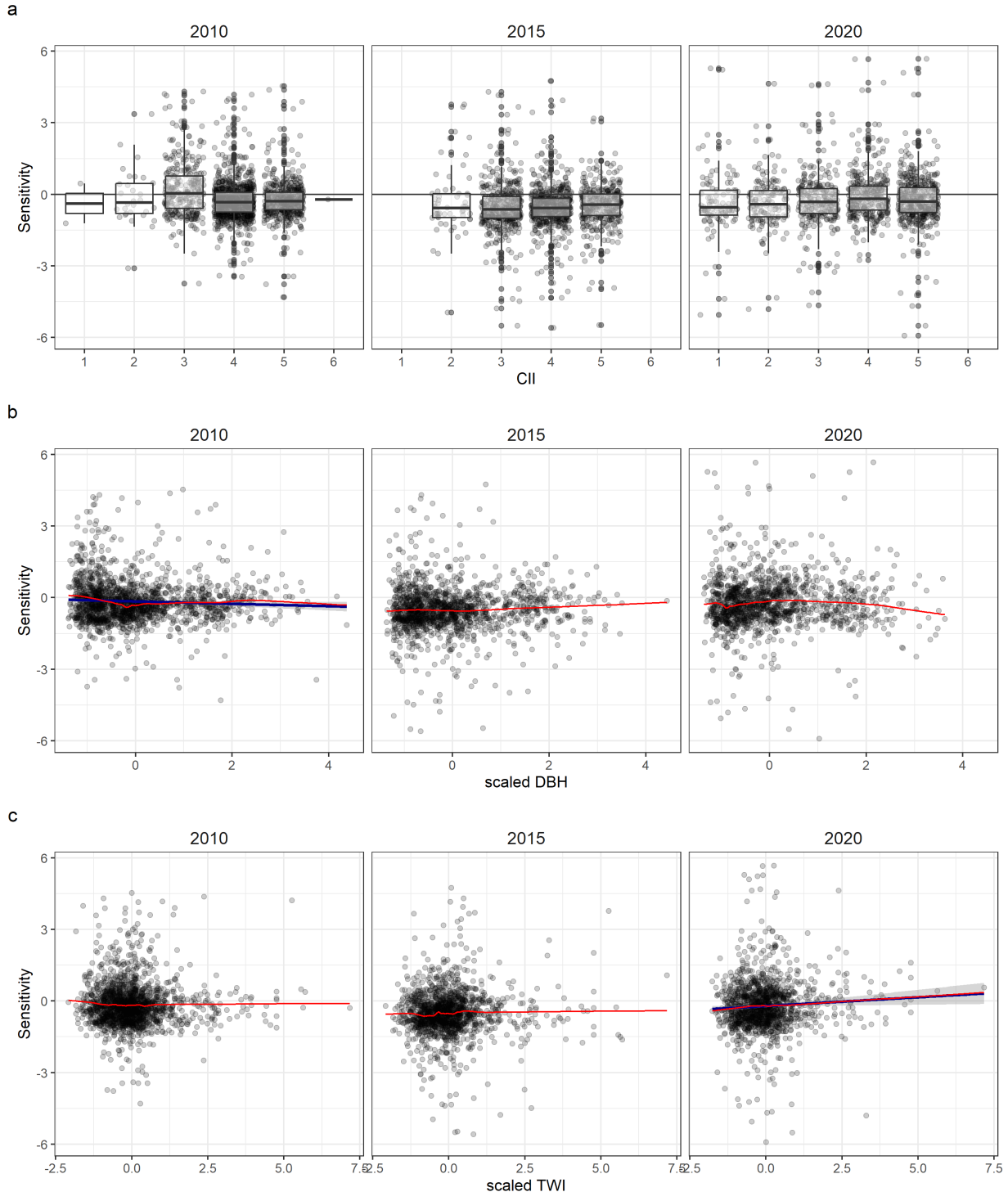


Figure S12: Distribution of raw sensitivity values across years and their relationship with DBH, CII and TWI. Blue lines are linear model fits for statistically significant relationships at $p < 0.05$. Red lines are Friedman's SuperSmooother fits for all.

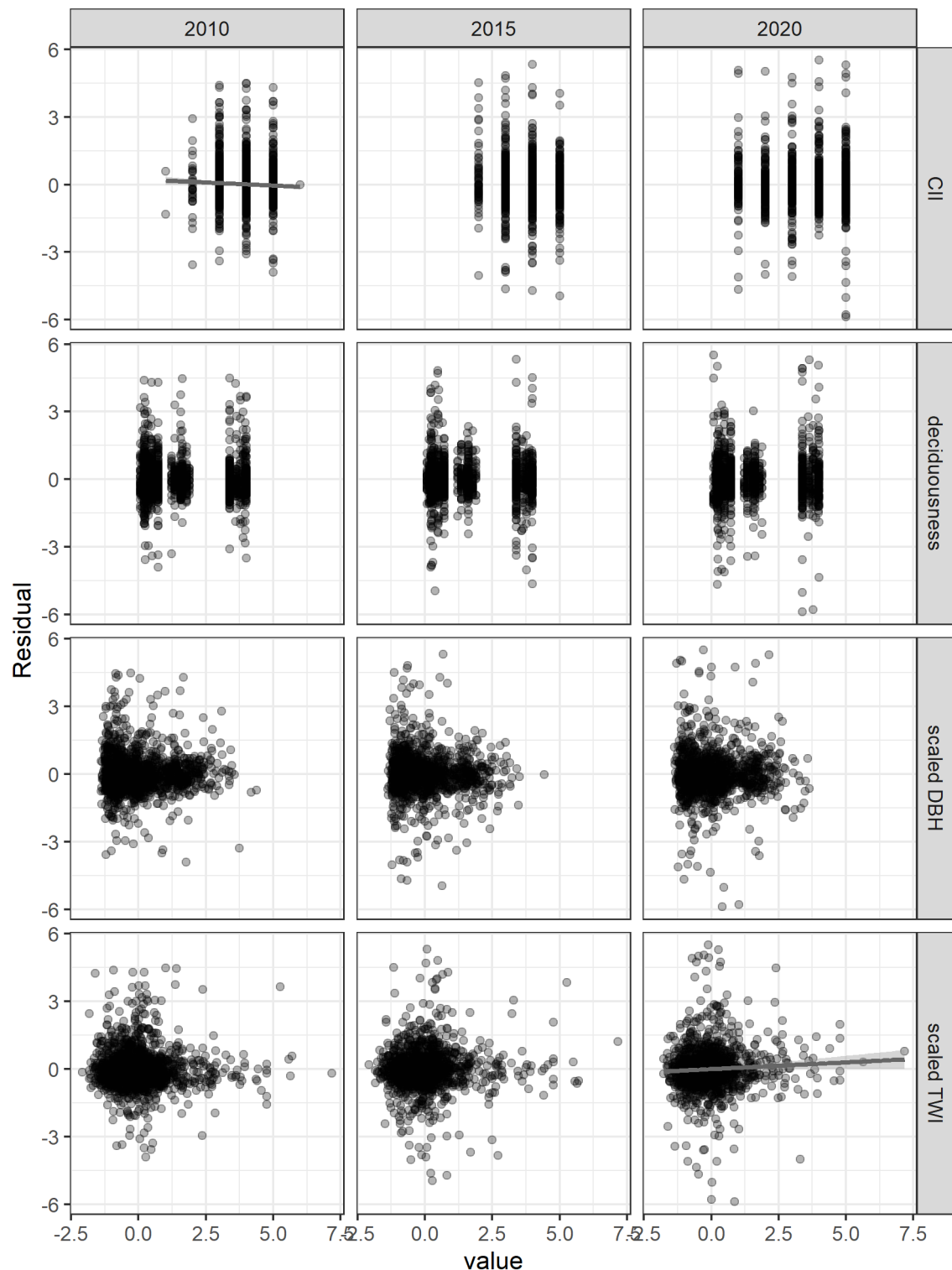


Figure S13: Distribution of residuals of species intercept models of sensitivity and their relationship with scaled DBH, TWI and CII and deciduousness. Grey lines are linear model fits for statistically significant relationships at $p < 0.05$. Species intercept model results are reported in main text.

Conditional dependencies

To analyse the influence of microenvironmental variables on growth sensitivity, we first created a Directed Acyclic Graph describing the relationships. The consistency of the DAG with the dataset, and our ability build causally interpretable models, is conditional on the numerical independence among some specific variable groups, as implied by the DAG structure. We identified these “testable implications” or “conditional independences” for this DAG using *dagitty* as $CII \perp\!\!\!\perp TWI$ and $DBH \perp\!\!\!\perp TWI$. We tested these correlations using the function *cor()* in R, with the simple criteria that a Pearson’s correlation coefficient <0.3 implies independence among variable pairs and causal relevance of the DAG.

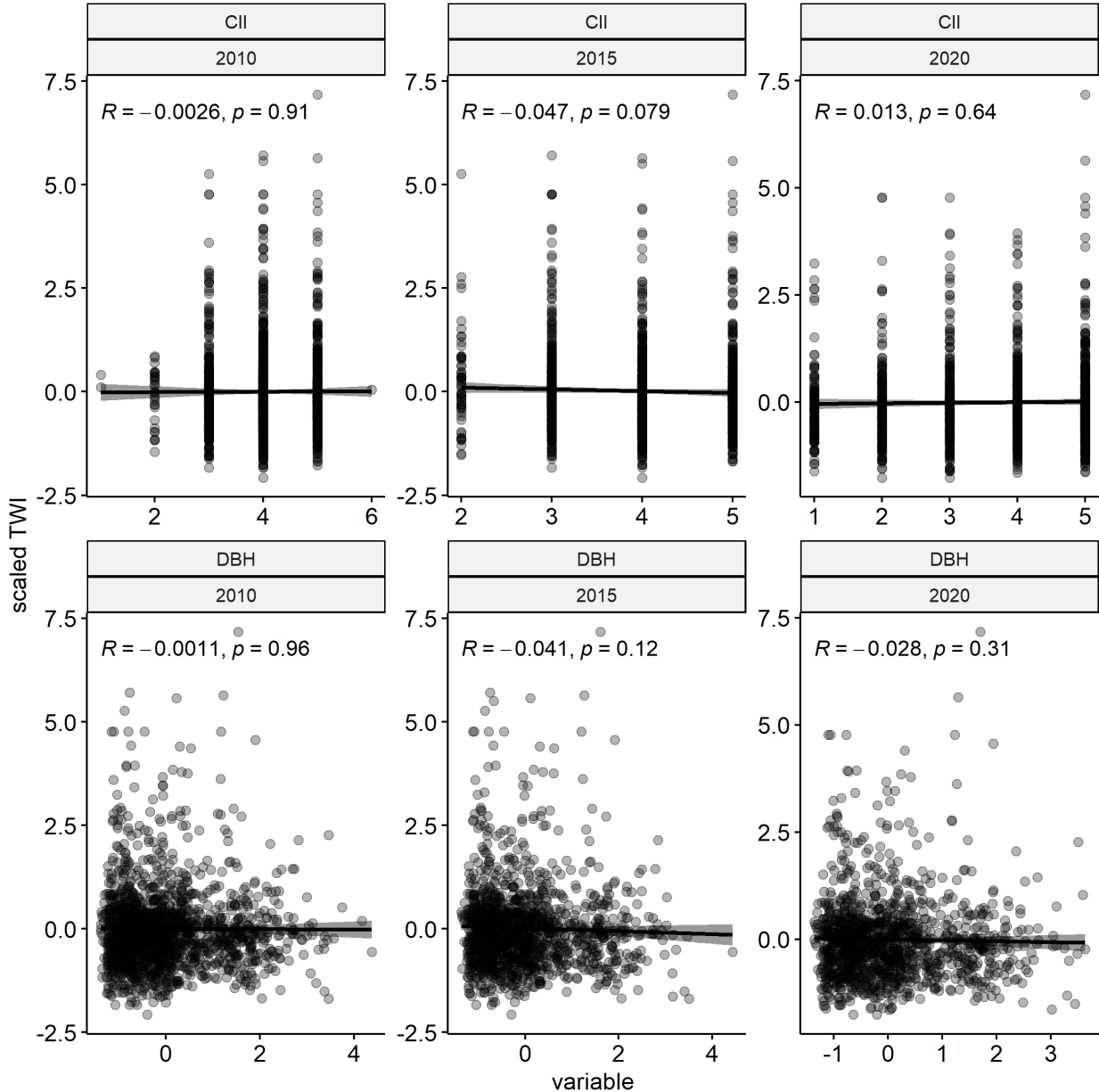


Figure S14: Testing correlations of variables across all individuals

There is low correlation between these two variable pairs across all individuals. We then tested conditional dependencies at the species level.

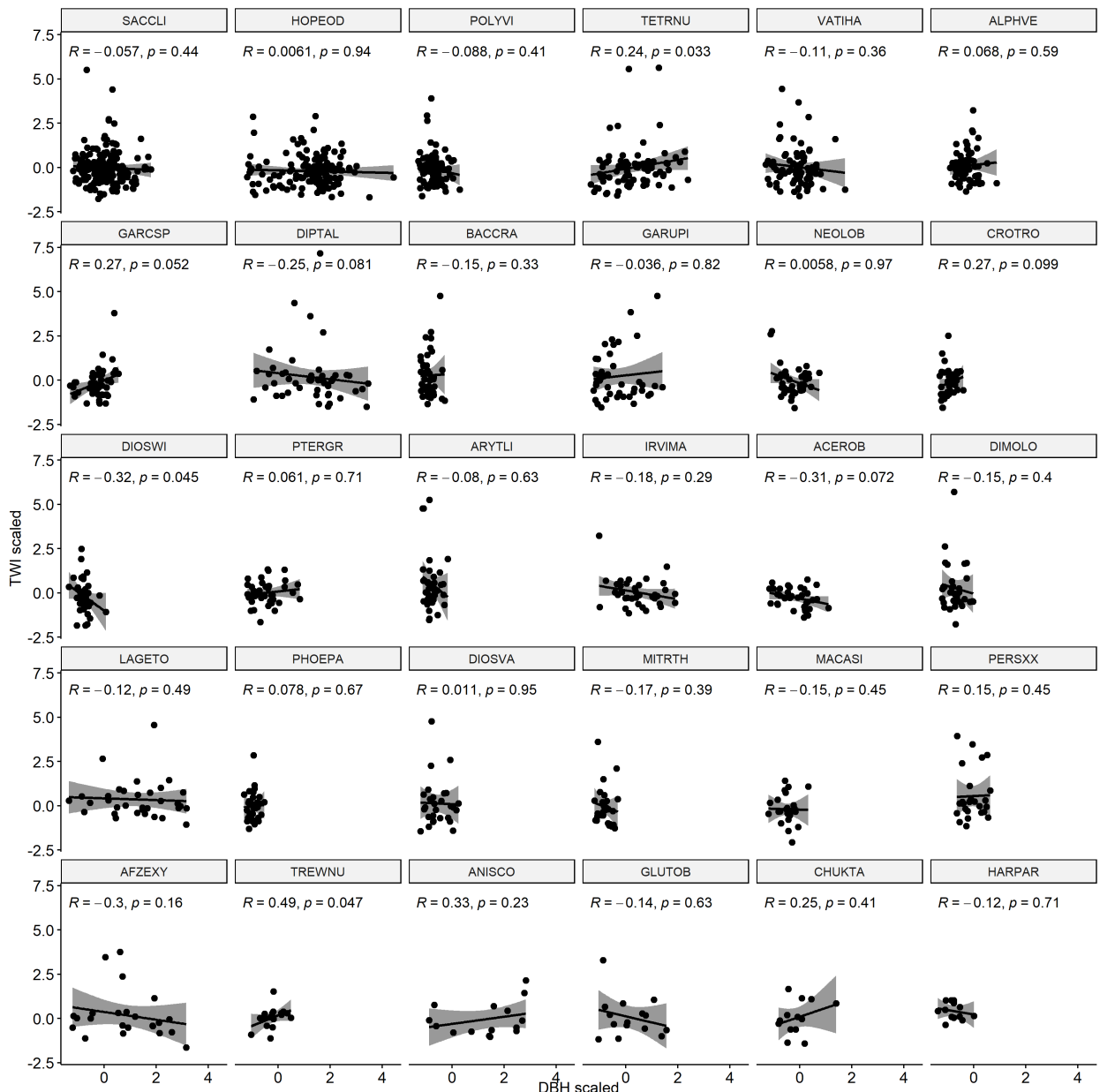


Figure S15: Testing correlations for $\text{DBH} \perp\!\!\!\perp \text{TWI}$ by species

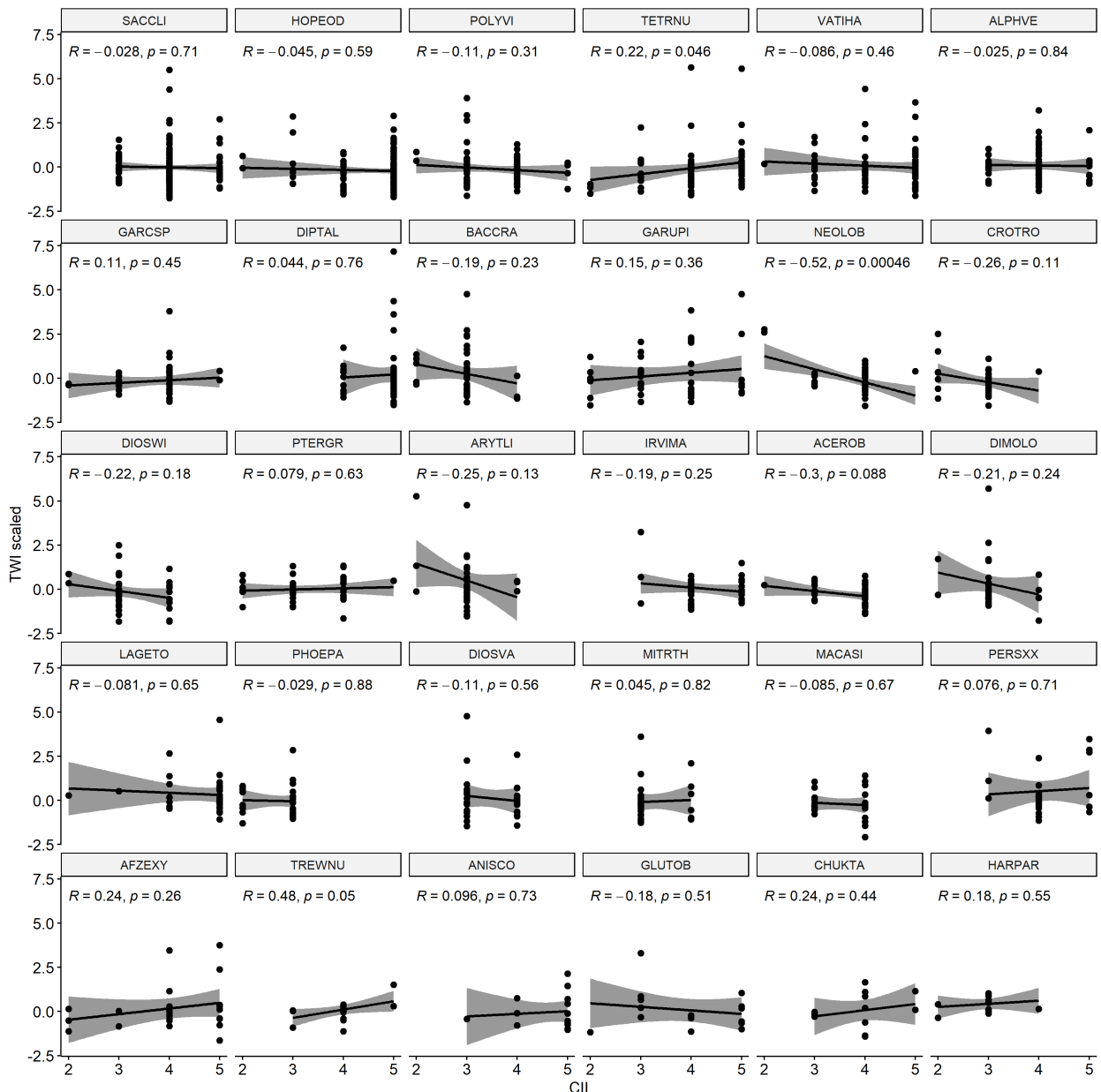


Figure S16: Testing correlations for $\text{CII} \perp\!\!\!\perp \text{TWI}$ by species

Most species (barring a few) had low correlation between these variables in our dataset, allowing us to proceed with analysis and interpretation.

Alternate models using Topographic Position Index

As an alternate measure of wetness to Topographic Wetness Index (TWI) that requires the total upslope area, we used Topographic Position Index (TPI), a localised convexity/concavity-based metric of water availability as a predictor. We calculated TPI using the package *spatialEco* (Evans & Murphy, 2023) using a circular buffer window of 1, 3, 5 and 7 pixels. Larger window sizes while providing a smoother surface on the plot, clip out larger portions of the plot margin where the window might bleed outside. We chose to use the 5-pixel version because of the balance between smoothness across the landscape and data loss.

TPI and TWI had better resolution in different parts of the wetness gradient, with TWI capturing larger resolution among wetter locations and TPI capturing larger resolution among drier locations. Interaction models of deciduousness with TPI showed qualitatively similar results with the TWI models across the three drought years.

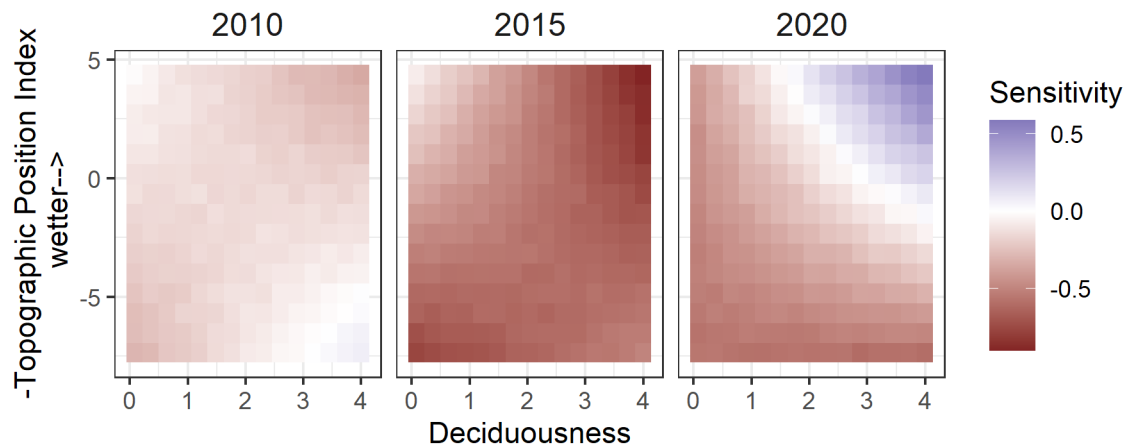
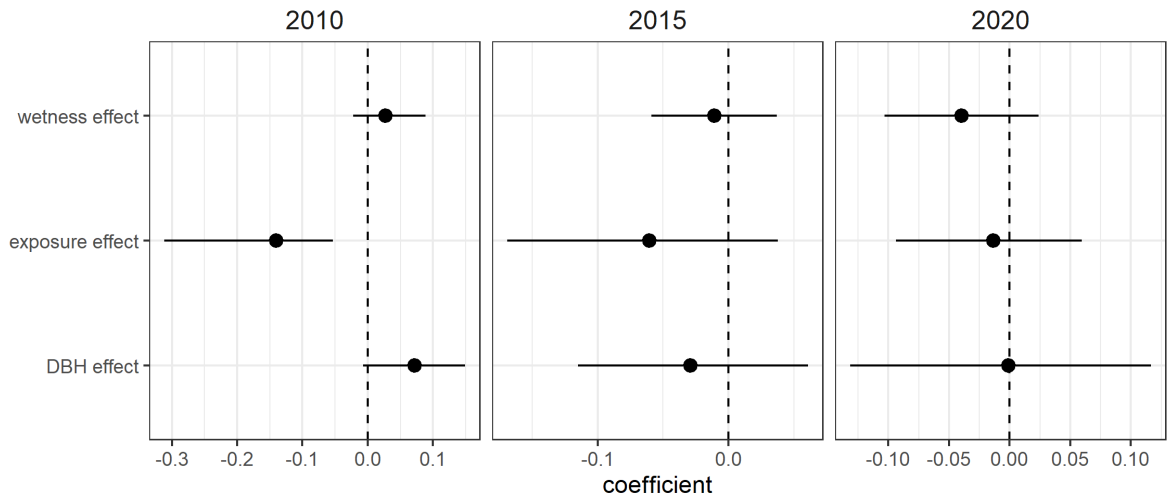


Figure S17: Correlation of modelled species sensitivities with Topographic Position Index

Similarly, models accounting for DBH and CII showed similar directional effects of wetness whether TWI or TPI was used. Please note that left to right represents wet to dry, given the way that TPI is calculated.

a



b

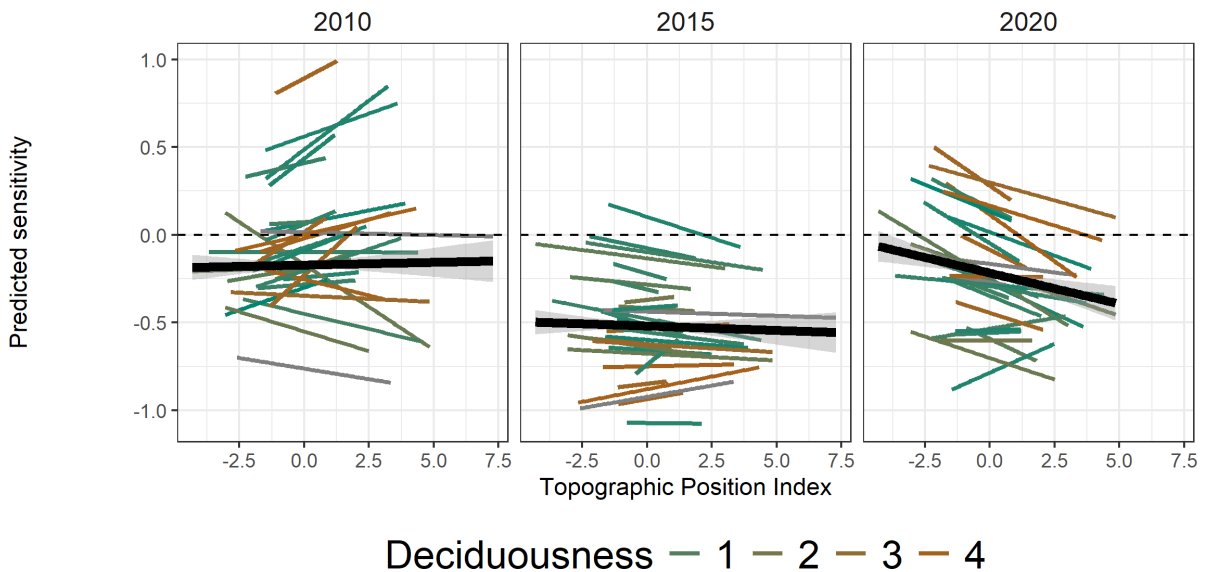
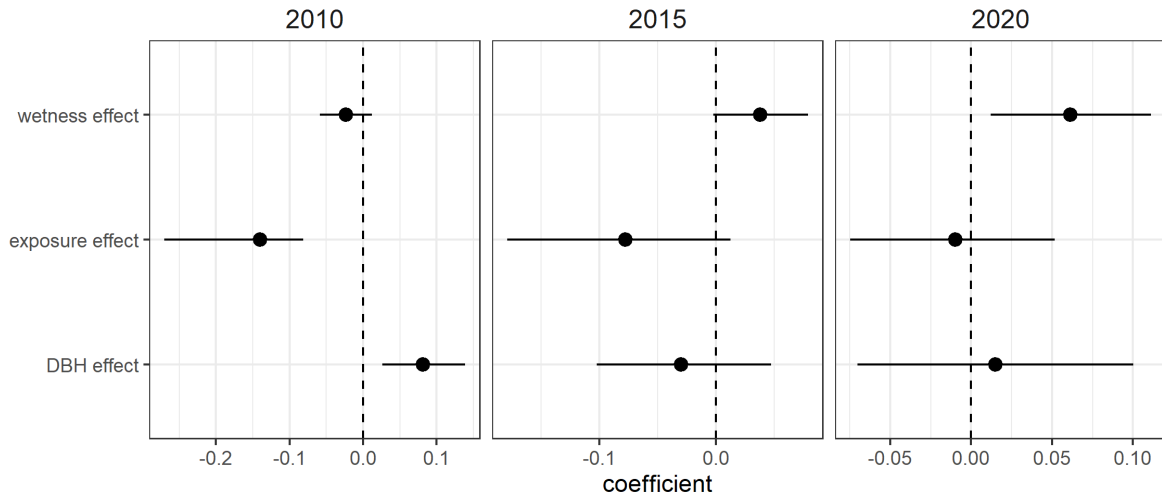


Figure S18: Model results from Bayesian causal model of sensitivity as a function of DBH, CII and TPI.

Alternate model using species random effect only on intercept

a



b

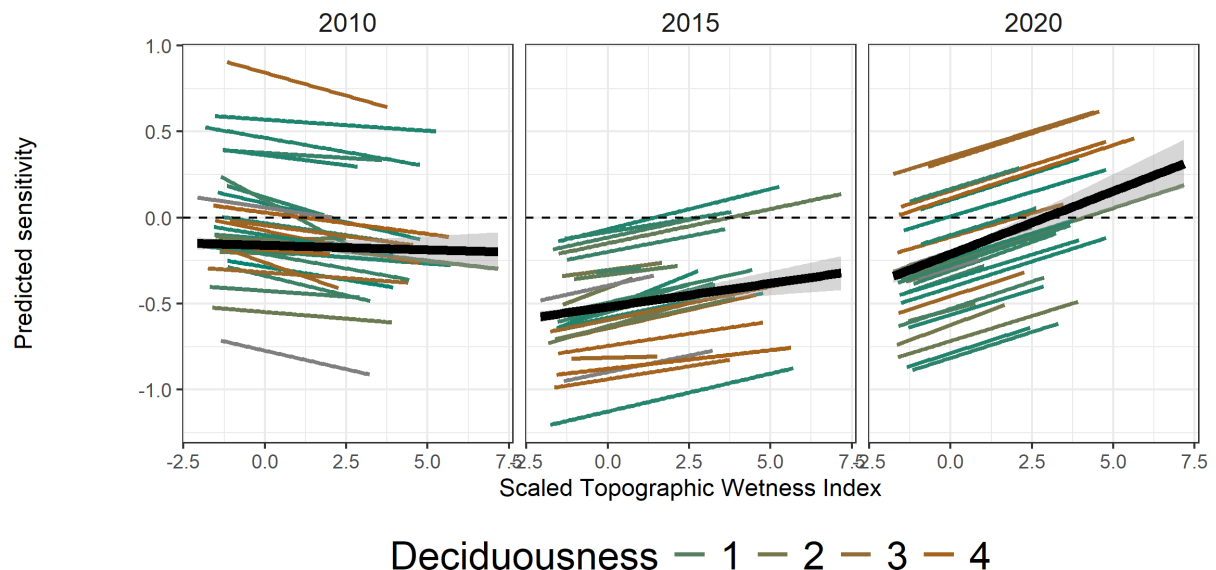


Figure S19: Model results from Bayesian causal model of sensitivity as a function of DBH, CII and TWI with species random effect only on intercept.

Alternate models as causal inquiries following backdoor criteria

For an alterate approach, we used a backdoor criteria approach as used in causal inquiry to test the effects of DBH, CII and TWI on sensitivity separately starting from a combined DAG. First, we specified the DAG on DAGitty (Textor *et al.*, 2016) in the same strcuture as described in Fig 5 in the main text. We then set sensitivity as the response variable, or “outcome”. For each variable - DBH, CII and TWI - whose causal effects we were interested in, we examined the minimum set of adjustment variables for each causal effect, by setting each of these as “exposure” one after the other and computing adjustment sets from DAGitty. This resulted in three different models to test the total causal effects:

For TWI: $sensitivity \sim TWI$

For CII: $sensitivity \sim CII$

For DBH: $sensitivity \sim DBH + CII$

We fit three different models on *brms*, with normal priors for sensitivity, TWI and DBH and a monotonic prior for CII. All models had a random effect of Species on both slopes and intercept. Results from the causal inquiries following backdoor criteria align very closely with the SEM-like Bayesian causal model.

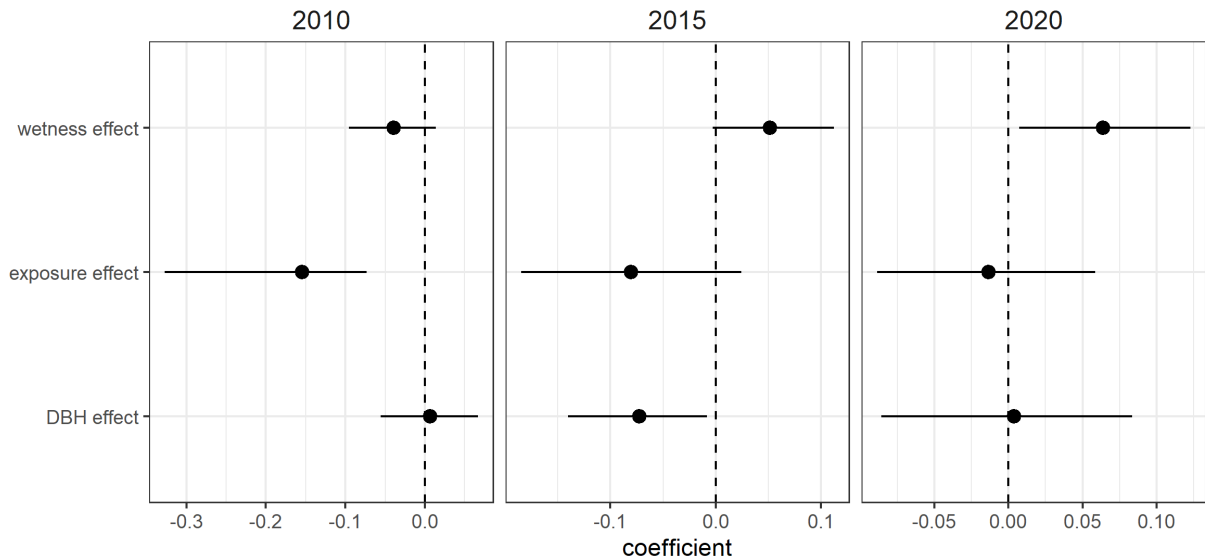


Figure S20: Model results from three independent causal inquiry models of sensitivity following backdoor criteria for total causal effect of DBH, CII and TWI with species random effect on intercept and slope.

References

- Evans JS, Murphy MA. 2023. *spatialEco*.
 Textor J, van der Zander B, Gilthorpe MS, Liśkiewicz M, Ellison GT. 2016. Robust causal inference using directed acyclic graphs: The R package ‘dagitty’. *International Journal of Epidemiology* **45**: 1887–1894.